MATERIALS PHYSICS AND MECHANICS RESEARCH ARTICLE

Submitted: August 28, 2024 **Revised: September 12, 2025** **Accepted: October 30, 2025**

Multi-physics simulation to estimate exposure time for microwave-assisted metallic cast

A. Kumar ✉, **A.K. Bagha**, **S. Sharma**

Dr. B. R. Ambedkar National Institute of Technology Jalandhar, Punjab, India

✉ ashishkumar.me.22@nitj.ac.in

ABSTRACT

Microwave casting utilizes microwave energy to heat and cast metallic materials. This technique is novel and efficient in comparison to traditional methods. This technique has been applied to cast various metallic materials. There are some factors like dielectric characteristics of processing material, casting setup design, and choices of susceptor and mold, that affect the microwave heating rate. Consequently, determining the optimal exposure time for cast experimentally can be challenging. To address this, simulation studies are valuable. This study involves finite element modeling of microwave casting experimental setup. Using finite element simulations, the exposure times are predicted that are required to cast various metallic powders (Ni, stainless steel SS-316, and Cu) under identical parametric conditions in an electromagnetic environment. The impacts of microwave heating are analyzed through electric field configuration, resistive losses, and thermal distribution within the applicator cavity. The electric field intensity is observed to be maximum (4.46 × 104 V/m) in the susceptor zone, resulting in the highest resistive losses (4.9 × 109 W/m^3) in that area. Under the specified conditions, the exposure times to cast Ni, SS-316 and Cu powder into dimensions of 150 × 35 × 3 mm^3, are predicted as 2280, 2080, and 1125 s respectively. Experimental results confirm these times with an average percentage error of 13.83 %, demonstrating a close correlation between predicted and actual exposure times.

KEYWORDS

microwave casting • exposure time • FE model • simulation

Acknowledgments. *The author(s) would like to thank and acknowledge Indian Science Technology and Engineering Facilities Map (I-STEM), a program sponsored by the Office of the Principal Scientific Adviser to the Govt. of India, for enabling access to COMSOL Multiphysics 5.6 software suite to carry out this work.*

Citation: Kumar A, Bagha AK, Sharma S. Multi-physics simulation to estimate exposure time for microwave-assisted metallic cast. *Materials Physics and Mechanics*. 2025;53(6): 130–144.
http://dx.doi.org/10.18149/MPM.5362025_10

Introduction

Over the years, materials have been fabricated through traditional casting processes and are extensively used for industrial applications [1,2]. In these processes, conventional heating sources are used to heat the materials from the exterior to the interior core. This results in several drawbacks, such as non-uniform heating, high energy consumption, long processing time, material wastage, and, most importantly, not being suitable to the environment [3]. Over the last two decades, researchers from all around the world have been trying to develop a novel technique that can provide advantages of energy efficiency, unique heating abilities, and an eco-friendly working environment; however, they are facing challenges. Microwave-assisted casting is an advanced manufacturing technique that offers numerous benefits over traditional methods. The conventional heating processes rely on conduction or convection to transfer heat from a source to a target. Whereas microwave heating directly converts energy into heat within the material

© A. Kumar, A.K. Bagha, S. Sharma, 2025.
Publisher: Peter the Great St. Petersburg Polytechnic University
This is an open access article under the CC BY-NC 4.0 license (https://creativecommons.org/li-censes/by-nc/4.0/)

itself. This method eliminates the need for heating furnaces and other heat transfer mediums. Microwaves are absorbed by the material, causing its particles to interact and generate heat throughout the entire volume, resulting in more uniform heating [4]. This efficient heating process reduces energy consumption and improves overall operational efficiency. Microwave-assisted casting offers significant energy advantages, with the required energy being only about one-third of that in conventional casting. Combined with direct volumetric heating, shorter processing times, and reduced heat losses, this highlights its superior energy efficiency. Additionally, microwave heating is relatively simple to implement, requires less setup compared to traditional methods, and produces less waste or hazardous by-products, making it a greener technology [5,6].

The electromagnetic waveform that has a frequency between 300 to 300 GHz is termed as microwaves. The microwave heating phenomenon relies on the principle of dielectric heating [7]. The depth of penetration (skin depth) of microwaves into materials, is crucial for effective microwave processing. For metallic materials, the skin depth is very small, so direct exposure to microwaves results in insufficient heating [8].

Earlier it was believed that processing metallic materials with microwave energy was impossible because metals reflect microwaves and do not interact effectively with them. To address this challenge, the concept of microwave hybrid heating (MHH) was developed [9,10]. This approach uses a susceptor [11–13], a microwave-absorbing material with a high dielectric loss factor. The susceptor is utilized to initially transfer heat to the metal until it reaches its critical temperature (T_c). Once the metal reaches this temperature, it begins to absorb microwaves effectively with increased penetration depth. Microwave-assisted metal casting uses microwave energy to melt and process metal-based materials. It can be classified into in-situ and ex-situ castings [14–17]. A variety of metals, alloys and metal matrix composites (MMCs) were cast through MHH are listed below in Table 1.

It is revealed from the literature that the casting of materials using microwave energy is dependent upon various process parameters such as casting setup design and geometry, dielectric characteristics of casting material and operating conditions [14]. Based on

Table 1. Parametric description of various microwave casts reported earlier

Sr. No.	Authors	Material	Weight / size, g/mm	Susceptor	Applicator frequency, GHz	Power, W	Exposure time, s
1.	Gangwar, et al. [18]	Alum. Alloys 6063/6063A	150	Silicon carbide (SiC)	2.45	900	700
2.	Kaushal [19]	MMC	50 × 12	Charcoal powder	2.45	900	900
3.	Lingappa, et al. [20]	Al 1050	250	Silicon carbide (SiC)	2.45	900	1200
4.	Mishra and Sharma [21]	AA 7039	–	Silicon carbide (SiC)	2.45	1400	930
5.	Mishra and Sharma [22]	Copper	–	Silicon carbide (SiC)	2.45	1400	900
6.	Shashank, et al. [23]	Brass	600	Silicon carbide (SiC)	2.45	900	1500
7.	Marahadige, et al. [24]	Brass	–	Silicon carbide (SiC)	2.45	3300	1020
8.	Ram, et al. [25]	SS-316	60 × 20 × 5	Charcoal powder	2.45	900	1200
9.	Singh, et al. [26]	MMC	50×20×6	Charcoal powder	2.45	900	1500
10.	Kumar, et al. [27]	MMC	–	Charcoal powder	2.45	900	350
11.	Pal, et al. [28]	MMC	–	Pulverized charcoal	2.45	900	1900
12.	Nandwani, et al. [29]	MMC	55 × 12 × 5	Activated charcoal	2.45	900	1200
13.	Kaushal, et al. [30]	MMC	–	Charcoal powder	2.45	900	660–1020

selected process parameters, the heating rate of specimens is also affected. Therefore, it is difficult to estimate the optimal exposure time for microwave cast experimentally. Moreover, experimental measurement of parameters like electromagnetic distribution, thermal history and heat transfer mechanism within the cavity is also challenging. In these cases, simulation studies can be more effective for predicting and understanding the complex multi-physics involved in microwave heating phenomena. Simulation tools can incorporate detailed models of these phenomena, allowing for a more comprehensive understanding and prediction of the heating behavior. Multi-physics coupled model can provide insights into how different parametric conditions influence the heating rate during the process [31].

In [32–36], FE simulations are successfully modelled and validated by researchers for microwave processing and melting of metallic materials using parametric variations. However, there is limited research reported on predicting the optimal exposure time for microwave casts of different sizes and materials. In this context, in this work, the FE simulation model of a microwave casting setup is designed through the COMSOL multi-physics tool. The FE model examines the MHH effects and predicts the exposure time required to cast different metallic powders (Ni, SS-316, and Cu) in an electromagnetic environment. The impacts of MHH are analyzed within the applicator cavity through electric field configuration, resistive heating, and thermal distribution. Based on these predicted exposure times, the specimens are cast experimentally using microwave casting. The study includes the comparison of the simulated outcomes with the experimental findings.

FE model

Microwave-assisted casting involves multi-physics phenomena, including electromagnetic field interactions and heat transfer. An FE model of microwave casting is developed using the COMSOL multi-physics tool [37]. This study involved creating a 3D geometry of the experimental setup by considering the actual experimental conditions. After the geometry is established, material properties are allocated to each component based on the actual specifications. The model geometry is then discretized into smaller elements to approximate the behavior of the entire system.

3D geometric model

Microwave-assisted casting experimental setup composed of microwave applicator and casting setup. Casting setup includes the metallic powder, mold, refractory brick, susceptor and masking brick. Figure 1 represents the schematic diagram of the casting setup.

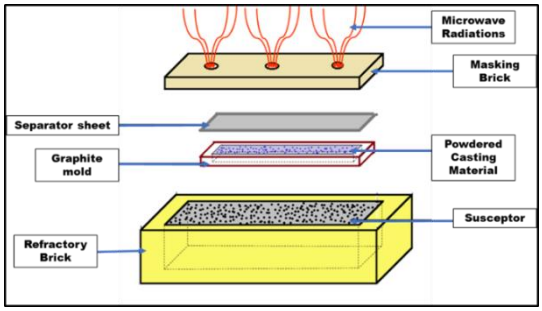

Fig. 1. Schematic diagram of refractory brick casting setup

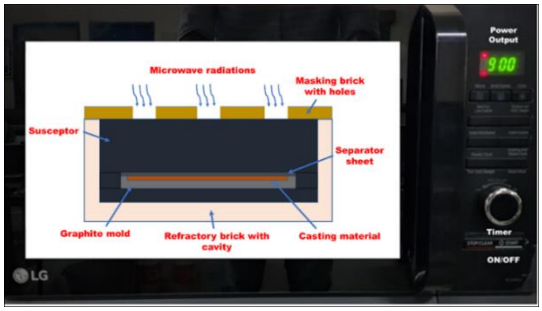

Fig. 2. Schematic diagram of experimental setup

To simplify the FE model, the following assumptions are taken into consideration (Fig. 2):

1. The waveguide and microwave cavity walls are constructed from stainless steel.
2. The microwave cavity is assumed to be filled with air.
3. The microwave oven operates at a frequency of 2.45 GHz and 900 W power output.
4. The port is excited by a transverse electric field.
5. The surrounding temperature is assumed to be 20 ºC.
6. The material properties are considered isotropic and homogeneous.
7. The dielectric and thermo-physical characteristics of the materials are assumed to be constant.
8. Mass transfer is disregarded in the study.
9. The powder material is modeled as a bulk or plate form to simplify the computational model and reduce complexity.

These simplified assumptions reduce computational complexity but may cause deviations in temperature distribution, heating uniformity, and exposure time. Ignoring mass transfer and modeling the powder as bulk can also lead to minor differences between simulated and experimental results.

Figure 3 represents the 3D geometric model of the microwave casting experimental setup modeled in COMSOL. A mold is designed with a cavity to hold the casting material. The mold is covered with the separator sheet to avoid the contamination of casting material through the susceptor. A refractory brick with a cavity is designed to contain a susceptor and prepared mold.

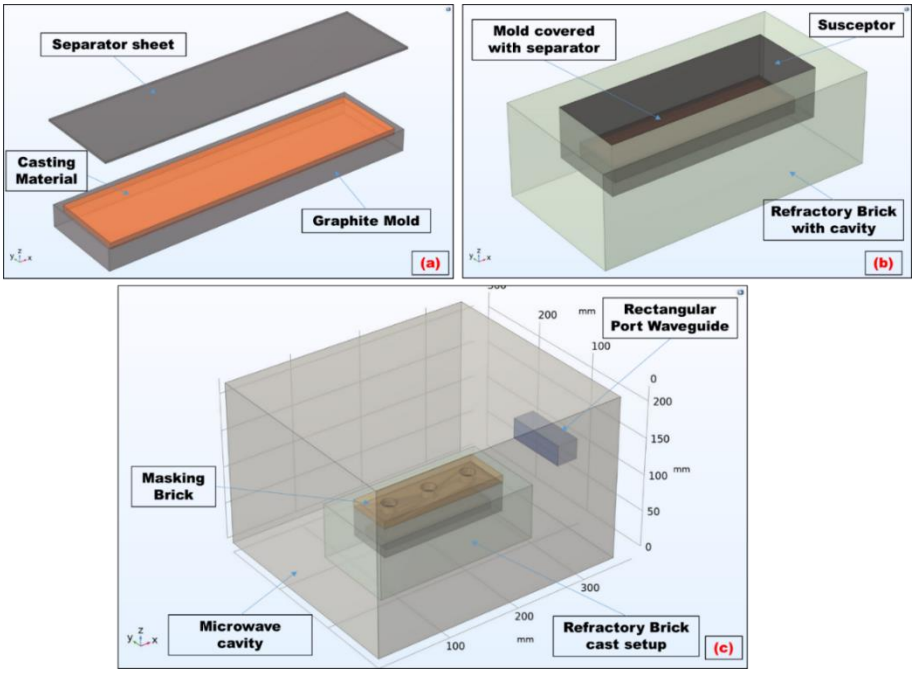

Fig. 3. 3D geometric model (a) mold and separator sheet, (b) refractory brick casting setup, (c) casting setup inside the microwave cavity

The refractory brick is covered with the masking brick with holes to allow selective microwave hybrid heating (SMHH). The complete refractory brick casting setup is placed at the optimized location within the applicator cavity. Microwave enters the cavity through rectangular port waveguide.

Table 2 displays the dimensional specifications for the components of the geometric model utilized in the experimental setup. The properties of materials are essential in microwave heating. Table 3 provides the input values for these properties in the simulated model. Relative permeability is assumed unity for all materials.

Table 2. Dimensions of the 3D geometric model

Geometry	Size, mm³
Waveguide port (TE_{10})	30 × 85 × 28
The cavity of applicator	345 × 300 × 200
Mold (cavity)	156 × 41× 10 (150 × 35 × 3)
Refractory brick (cavity)	224 × 114 × 75 (174 × 62 × 40)
Masking brick (holes)	174 × 62 × 10 (3 × Ø 25 × 10)
Separator sheet	156 × 41 × 1

Table 3. Material properties [11,32,38]

Material properties	Density (ρ), kg/m³	Electrical conductivity (σ), S/m	Relative permeability (μ_r)	Relative permittivity (ε_r)	Heat capacity at constant pressure (C_p), J/(kg·K)	Thermal conductivity (k), W/(m·K)
Ni Powder	8902	14577	1	1	440	90.9
Charcoal powder	1300	0.02	1	2.5	4186.8	0.478
Air	1	0	1	1	0	0
Stainless steel	7850	1.339e6	1	1	490	16.5
Alumina	2770	1e-14	1	4.3	885	0.32
Graphite	2100	1300	1	15	830	470
Cu powder	8700	5.998e7	1	1	385	400

Governing equations

MHH is dictated by Maxwell's electromagnetic wave equation. The following equation governs the propagation of microwaves from the port to the cavity of the applicator.

$$\nabla \times \mu_r^{-1}(\nabla \times E) - k_0^2\left(\varepsilon_r - \frac{j\sigma}{\omega\varepsilon_0}\right)E = 0, \quad (1)$$

where E is the electric field (V/m), k_0 is wave number of free space, ε_r is relative permittivity, ε_0 is the permittivity of free space, μ_r is the relative magnetic permeability, and σ is an electrical conductivity (S/m).

The relative permittivity is given as:

$$\varepsilon_r = \varepsilon' - j\varepsilon", \quad (2)$$

where ε' and ε'' are the dielectric constant and energy factor, respectively.

The relative magnetic permeability of any material during magnetization is calculated as:

$$\mu_r = \mu' - \mu", \quad (3)$$

where μ' and μ'' are magnetic field penetration into the material and magnetic loss tangent, respectively.

When an electromagnetic wave interacts with any dielectric material, the wave energy gets converted into heat can be defined as follows:

$$Q_e = Q_{rh} + Q_{ml}, \quad (4)$$

where Q_e, Q_{rh} and Q_{ml} are electromagnetic losses (W/m^3), resistive heat losses (W/m^3) and magnetic losses (W/m^3) respectively.

The resistive Q_{rh} and magnetic heat losses Q_{ml} are computed through the following:

$$Q_{rh} = \frac{1}{2} Re(J \cdot E^*), \quad (5)$$

where ω is angular frequency, J is current density (A/m^2), R_e is the Nusselt number, and E^* is electric field intensity;

$$Q_{ml} = \frac{1}{2} Re(i\omega B \cdot H^*), \quad (6)$$

where H^* and B represents the magnetic field intensity (A/m) and magnetic flux density (Wb/m^2), respectively.

The average power P_{avg} required for the conversion of electric energy into heat energy is given by the following equation:

$$P_{avg} = tan\,\delta\, E_{avg}, \quad (7)$$

where

$$E_{avg} = \frac{1}{2} \varepsilon_0 \varepsilon' E^2. \quad (8)$$

Meshing and boundary conditions

Discretizing the entire model geometry into numerous small segments is referred to as meshing. These subdivisions typically have simple shapes, such as triangles, quadrilaterals, tetrahedrons, or hexagons. To achieve convergence and accurate simulation results, mesh size is a critical factor. Mesh quality is assessed on a scale from 0 to 1, where 1 represents perfectly regular or structured elements, and 0 indicates distorted elements.

Figure 4(a) illustrates the mesh geometry. In the present FE model, a physics-controlled mesh is preferred over a user-defined mesh to ensure high-quality and accurate meshing. The physics-controlled mesh offers a range from extremely coarse to extremely fine mesh quality. For the current model, a fine mesh quality has been chosen. The finalized geometry includes 12 domains, 81 boundaries, 156 edges, and 96 vertices. The mesh comprises 760 edge elements, 4,992 boundary elements and 23,720 domain elements. The mesh quality statistics was evaluated, yielding an average elemental quality value of 0.6602, which, according to literature, falls within the acceptable range for achieving numerically accurate simulation results [11,12]. Figure 4(b) represents the mesh quality stat for the current FE model.

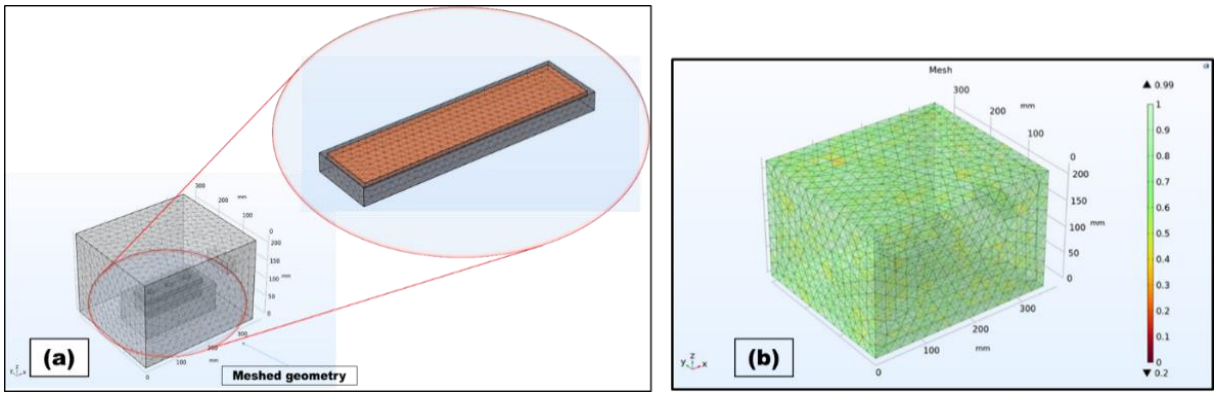

Fig. 4. (a) Mesh geometry; (b) mesh quality statistics for fine meshing

After completing the meshing process, boundary conditions are applied to the FE simulation model. Figure 5 represents the impedance and port boundary conditions [9,34,39]. As microwaves interact with the walls of the applicator cavity, they penetrate through the skin depth of the metallic material. In this simulation study, metallic walls of the applicator cavity are assigned as an impedance boundary conditions. The port boundary condition is assigned to the waveguide through which the microwave enters the cavity of the applicator.

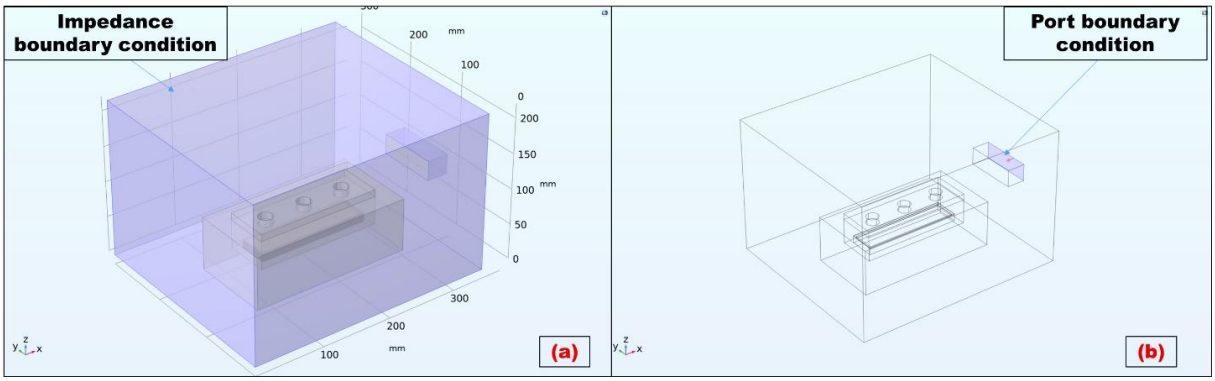

Fig. 5. (a) Impedance boundaries; (b) port boundary

Experimental study

This section describes the experimental process used to achieve microwave casting. Table 4 outlines the parameters used in the experimental process for microwave-assisted casting.

Table 4 Microwave casting process parameters

Process parameters	Overview
Microwave-type	Domestic microwave oven (Make: LG, MC3286BLT)
Cast specimen material	Ni, SS-316 and Cu powder
Power output (frequency)	900 W (2.45 GHz)
Surrounding temperature	20 °C
Susceptor	Powdered activated charcoal (AR)
Mold, separator sheet	Graphite
Refractory and masking brick	Alumina

Figure 6 represents the experimental setup which is used to achieve the microwave casting. A household microwave oven is utilized as a source of microwave energy for microwave metallic cast. To cast metallic materials using the MHH approach, a refractory brick casting setup is designed. In this work, fine metallic powders of Ni, SS-316 and Cu are taken as a cast material. The metal powder is packed in a microwave-absorbing graphite mold. A thin layer of refractory coating is applied to the interior surface of the mold to prevent the specimen from sticking. The graphite separator sheet (~ 1 mm thick) serves as a barrier between metallic powder and susceptor. Activated charcoal AR powder (molecular mass of 12.01 g/mol, density of 1.8–2.1 g/cm^3) is taken as susceptor. Activated charcoal powder is taken as a susceptor due to its high dielectric loss, thermal stability, cost-effectiveness, and easy of availability. The cavity of the alumina brick is used to contain the mold and the susceptor. The prepared mold is correctly positioned within the

cavity of the refractory brick and is surrounded by susceptor material. To facilitate SMHH, the cavity filled with the susceptor is then covered with masking alumina bricks with cylindrical openings. The cast setup is placed at the optimal location within the microwave oven to begin the heating process.

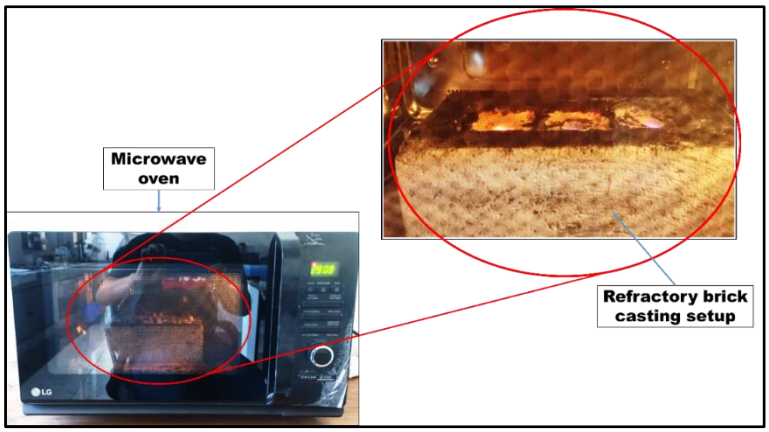

Fig. 6. Experimental setup

Results and Discussion

Simulation results

Firstly, the results in the form of electric field intensity, resistive losses, and thermal profile, obtained from the FE simulation are explained. Then the thermal profiles are compared for the different metallic casts including Ni, SS-316 and Cu.

Electric field distribution

As microwave radiations are the standing waveform; therefore, when these waves encounter any target, anti-nodal and nodal positions are developed. Nodal positions tend to cold spot regions or no heating zones and anti-nodal corresponds to the hot spot zones where the maximum heating takes place. The distribution of the electric field helps in predicting the optimum place to locate the casting setup inside the cavity to maximize

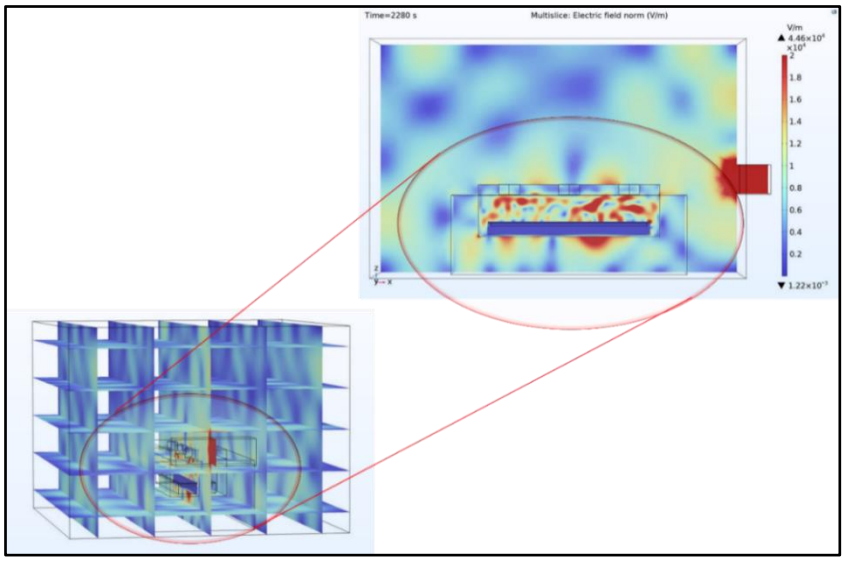

Fig. 7. Distribution of electric field

the microwave heating of the metallic cast [33,40]. The distribution of the electric field during the casting process is represented in Fig. 7, when the casting setup is located at the centremost location of the applicator cavity. The maximum intensity of the electric field is represented in red color and blue color represents the minimum electric field region. The maximum electric field strength is observed in the susceptor zone with a value of 4.46×10^4 V/m. This maximum electric field strength is likely to enhance the heating of this zone. In the free space of the applicator cavity, the value of electric field intensity is minimum as 1.22×10^{-3} V/m.

Resistive losses

The amount of energy transformed into heat energy through the absorber material is termed as resistive or joule heating. It is also responsible for heat dissipation through microwave-absorbing material. Figure 8 represents the resistive heating contour for the susceptor heating. It was observed that the resistive heating loss is maximized (4×10^9 W/m^3) within the susceptor zone. Therefore, in this zone, the maximum amount of energy of interaction between microwave and particles of charcoal powder is converted into heat. In the other domains such as microwave cavity filled with air, refractory brick and masking brick, zero losses as observed due to their non-interactive behavior with microwaves. This resistive heating phenomenon highlights the significance of SMHH.

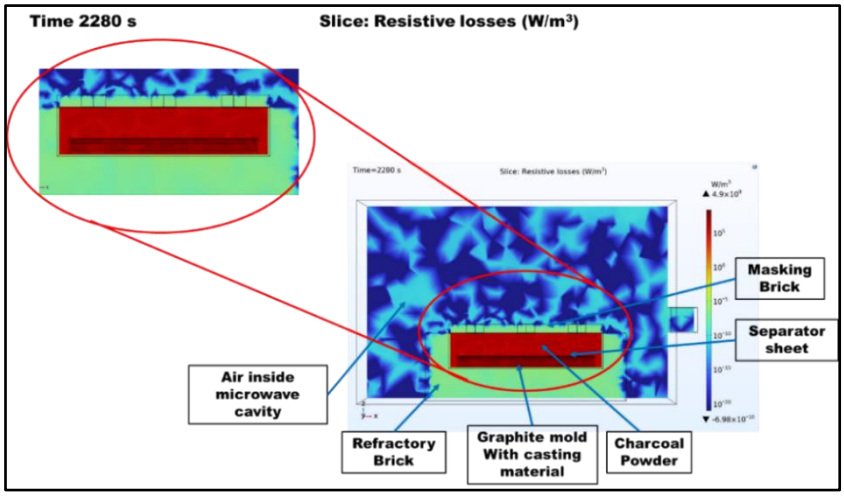

Fig. 8. Resistive heating (W/m^3)

Thermal profile

The simulation results of the thermal profile of the susceptor domain undergoing through microwave heating process are represented in Fig. 9. The thermal profiles have been plotted at four random time intervals of 360, 720, 1440 and 2280 s.

Figure 9 shows that the susceptor heats up more rapidly near the openings in the masking brick, which allows microwave radiation to enter the cavity. This illustrates the significance of SMHH. Due to interactions of microwaves with susceptor, there is a rapid increase in its temperature. The temperature of the susceptor reached around 1560 °C in 2280 s. The increased temperature of the susceptor helps in transferring the heat to the metallic powder through graphite mold via a conductive mode of heat transfer.

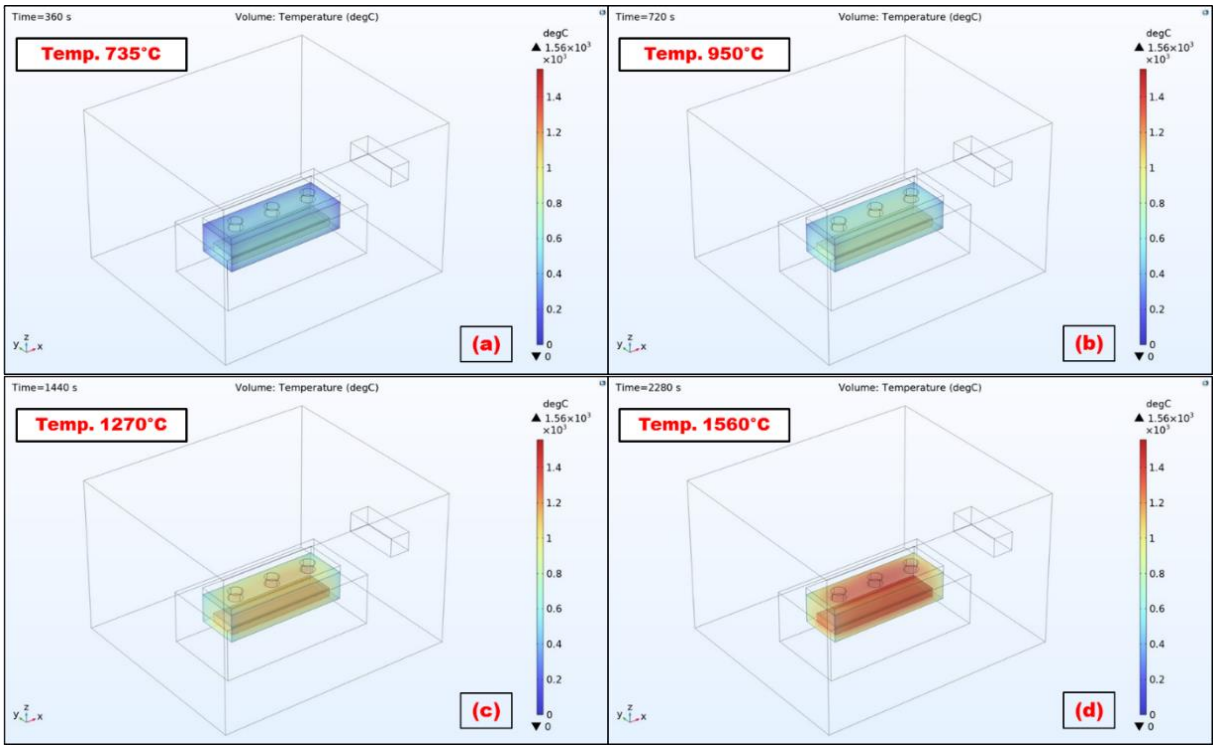

Fig. 9. Temperature distribution of charcoal inside the cavity at: (a) 360 s; (b) 720 s; (c) 1440 s; (d) 2280 s

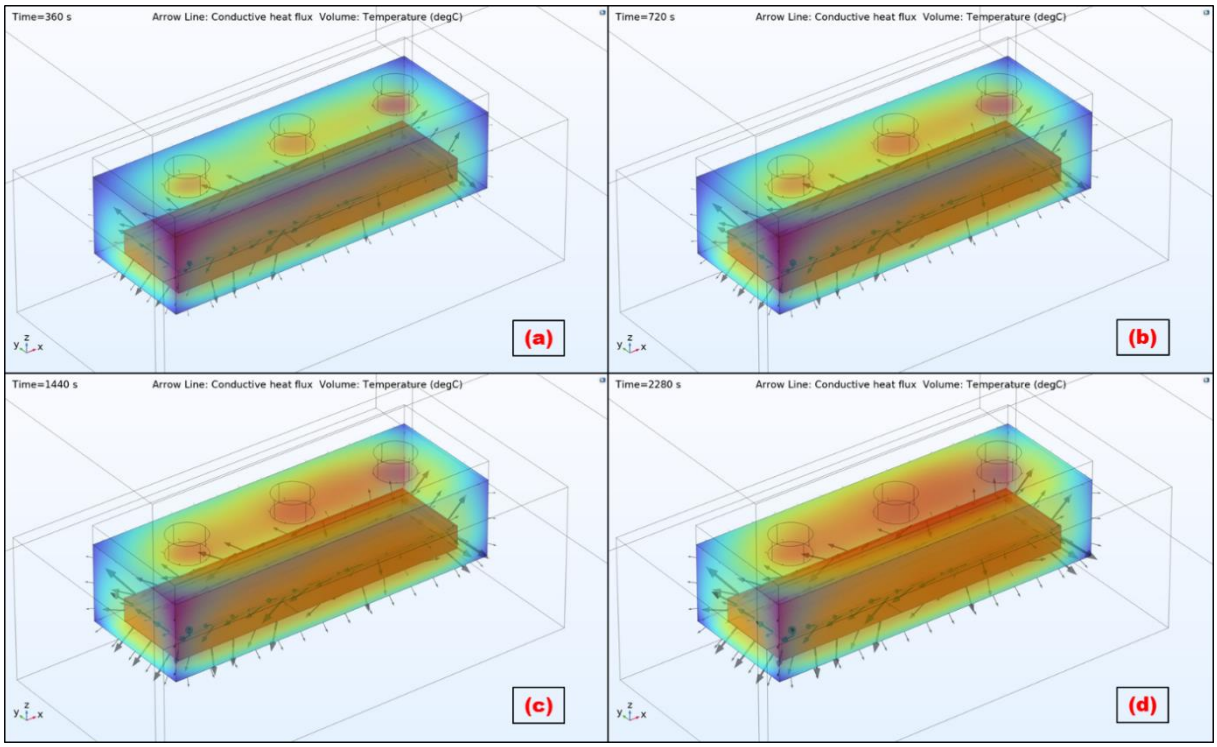

Fig. 10. Conductive heat transfer in susceptor domain at: (a) 360 s; (b) 720 s; (c) 1440 s; (d) 2280 s

The analysis of Fig. 10 illustrates the volumetric heating of the susceptor domain and the conductive flow of heat transfer through the susceptor inside the cavity. The black arrows indicate the direction of conductive heat flux, with the length of the arrow representing the magnitude of heat transfer. It is observed from Fig. 10 that the length of arrows increases with the increased temperature of the susceptor. This indicates that

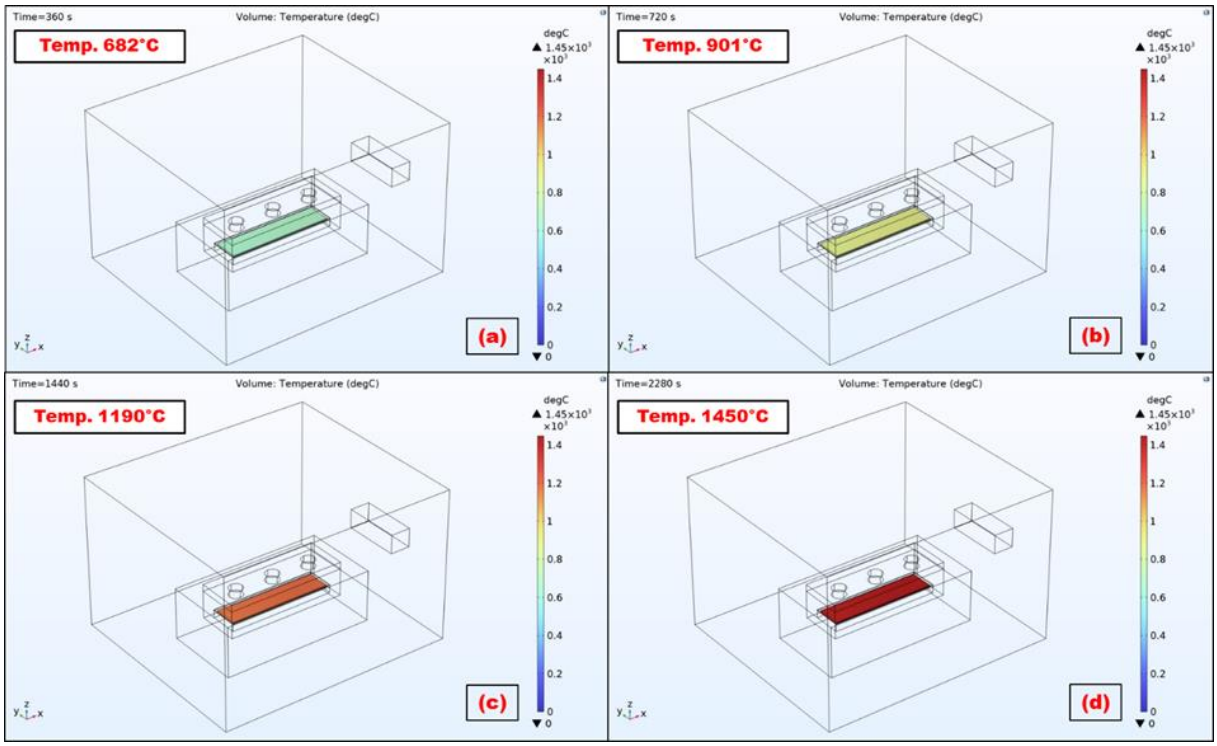

Fig. 11. Volumetric temperature distribution of Ni cast at: (a) 360 s; (b) 720 s; (c) 1440 s; (d) 2280 s

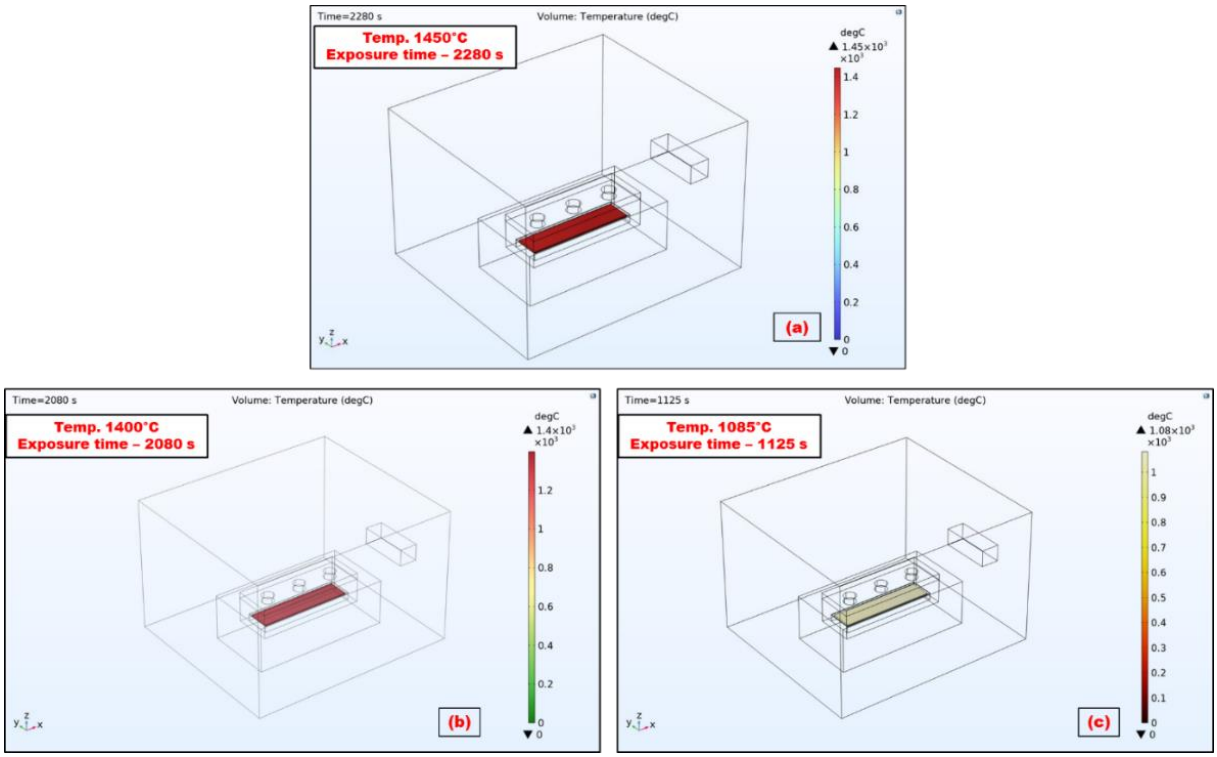

Fig. 12. Thermal profile for metallic cast: (a) Ni; (b) SS-316; (c) Cu

the magnitude of heat transfer through the susceptor rises with its temperature. The conductive heat transfer helps in raising the temperature of metallic powder inside the mold. As a result, the penetration depth of metallic powder to microwaves gets increased and it also starts absorbing the microwaves. The simulation results of thermal profile of

Ni powder undergoing through microwave heating process is represented in Fig. 11. According to the simulation results, the volumetric temperature of Ni cast approaches its melting point, approximately 1450 ºC, within 2280 s. The uniform heating is observed throughout the complete volume of the cast at these different time intervals. This highlights the significance of volumetric heating through microwave energy.

The MHH simulations are performed for SS-316 and Cu cast specimens using the same FE model. The properties of SS-316 and Cu powder are assigned instead of Ni Powder. For simulation, the properties of SS-316 powder are taken same as that of stainless steel used for cavity wall. The MHH effects in the form of electric field strength, and resistive losses are observed to be unaffected with change in cast material properties. Figure 12 represents the temperature profiles of Ni, SS-316 and Cu cast specimens corresponding to their melting temperatures. The simulation results reveal that uniform heating is achieved across the entire volume of all three cast specimens in the electromagnetic environment. The melting temperature of Ni, SS-316 and Cu cast specimens is achieved in 2280 s, 2080 s, and 1125 s respectively.

Fabrication of metallic cast using microwave casting

The Ni, SS-316, and Cu powders have been effectively cast utilizing a custom-designed refractory brick casting experimental setup. The setup is positioned within the applicator and the maximum power level is activated. Once the power is activated, the susceptor begins to absorb the microwave radiation. As a result, the susceptor starts to heat up. The heat produced by the interaction between microwaves and the susceptor causes a temperature increase in the metallic powder within the mold through conduction. As the temperature of metallic powder reaches its critical value, it also begins to absorb the microwave radiation with increased skin depth. The hybrid heating of metallic powder using susceptor and microwave radiation helps in reaching the melting temperature of the cast. The applicator power is switched off after reaching the optimum exposure time. The setup is cooled within the applicator to achieve proper bonding during solidification. The specimens cast using microwave radiation with their exposure time and sizes are discussed in Table 5.

Table 5. Sizes and exposure time for casts

Sr. No	Material	Size, mm^3	Exposure time, s	Metallic cast
1	Ni powder	120 × 32 × 2	1980	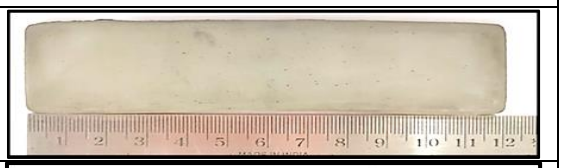
2	SS-316 powder	148 × 33 × 2	1740	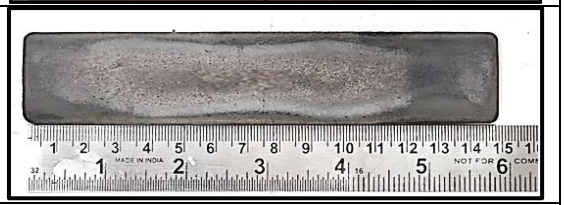
3	Cu powder	135 × 32 × 2	1260	

In microwave-assisted casting, Cu exhibits a shorter exposure time. This is primarily due to its high thermal conductivity and electrical conductivity, which enable faster heat transfer and more efficient energy absorption from the susceptor. In contrast, Ni and SS-316 have lower thermal conductivities and higher specific heat capacities, causing slower temperature rise and requiring longer exposure times to achieve complete melting.

Comparison of simulated and experimental exposure time

Table 6 represents the comparison of experimental and simulated exposure time for different cast specimens including Ni, SS-316 and Cu. It is observed from Table 6 that experimental and simulated exposure time for different metallic casts shows a close co-relation. The percentage error between experimental and simulated exposure time for Ni, SS-316 and Cu cast are observed as 13.15, 16.34 and 12.00 % respectively. The average percentage error is measured as 13.83 %. The deviation arises from using idealized material properties and modeling the powder as a homogenized bulk, neglecting porosity, particle morphology, and microstructural evolution. The FE model assumes isotropic and constant dielectric and thermo-physical properties, ignoring temperature-dependent variations. Additionally, the use of simplified boundary conditions and modeling assumptions may further limit the ability of FE model to fully capture the microwave-thermal interactions and real experimental conditions of the MHH process.

Table 6. Comparison of simulated and experimental exposure time

Sr. No	Metallic 9owder	Size of experimental cast, mm^3	Size of simulated cast, mm^3	Experimental exposure time, s	Simulated exposure time, s	Percentage error, %
1	Ni	120 ×32 × 2	150 × 35 × 3	1980	2280	13.15
2	SS-316	148 × 33× 2	150 × 35 × 3	1740	2080	16.34
3	Cu	136 × 32× 2	150 × 35 × 3	1260	1125	12.00

Conclusions

This study explores the microwave casting of metallic powders using an energy-efficient microwave heat source. An FE model of the experimental setup was created to predict the optimal exposure time for cast within the electromagnetic environment. Analysis of the simulation results indicated that the highest concentrations of electric field intensity are detected in the susceptor zone. The maximum electric field strength was recorded at 4.46×10^4 V/m. This high electric field strength increases heating in the susceptor zone through microwave irradiation, resulting in maximum resistive losses of 4.9×10^9 W/m^3 in that area. Consequently, conductive heat transfer through the susceptor raises the temperature of the metallic powder inside the mold. The simulations demonstrated that as the temperature of the susceptor increases, the magnitude of heat transfer through the susceptor to metallic powder also rises. The FE model accurately predicted the exposure times needed to cast various metallic powders. Experimental validation confirmed these predictions, showing a strong agreement between simulated and actual exposure times, with an average percentage error of 13.83 %. This demonstrates the effectiveness of the simulation in optimizing microwave casting processes and highlights its potential to improve efficiency and accuracy in metal casting applications.

CRediT authorship contribution statement

Ashish Kumar: writing – review & editing, writing – original draft; **Ashok K. Bagha**: writing – review & editing; **Sumit Sharma**: writing – review & editing.

Conflict of interest

The authors declare that they have no conflict of interest.

References

1. Kashyap S, Tripathi H, Kumar N. Mechanical properties of marble dust reinforced aluminum matrix structural composites fabricated by stir casting process. *Materials Physics and Mechanics.* 2022;48(2): 282–288.
2. Sulardjaka S, Nugroho S, Iskandar N. Mechanical properties of AlSiMg/SiC and AlSiMgTiB/SiC produced by semi-solid stir casting and high pressure die casting. *Materials Physics and Mechanics.* 2021;47(1): 31–39.
3. Salonitis K, Zeng B, Mehrabi HA, Jolly M. The Challenges for Energy Efficient Casting Processes. *Procedia CIRP.* 2016;40: 24–29.
4. Mishra RR, Sharma AK. Microwave-material interaction phenomena: Heating mechanisms, challenges and opportunities in material processing. *Composites Part A: Applied Science and Manufacturing.* 2016;81: 78–97.
5. Bhoi NK, Singh H, Pratap S, Jain PK. Microwave material processing: A clean, green, and sustainable approach. In: Kumar K, Zindani D, Davim P. (eds.) *Sustainable Engineering Products and Manufacturing Technologies.* Academic Press; 2019. p.3–23.
6. Kaushal S, Singh S, Bohra S, Gupta D, Jain V, Kapoor M. Sustainable microwave processing and surface characterization of powdered tungsten reinforced copper metal matrix (Cu-Wx) castings. *Results in Surfaces and Interfaces.* 2024;16: 100249.
7. Thostenson ET, Chou TW. Microwave processing: fundamentals and applications. *Composites - Part A: Applied Science and Manufacturing.* 1999;30(9): 1055–1071.
8. El Khaled D, Novas N, Gazquez JA, Manzano-Agugliaro F. Microwave dielectric heating: Applications on metals processing. *Renewable and Sustainable Energy Reviews.* 2018;82: 2880–2892.
9. Lingappa SM, Srinath MS, Amarendra HJ. Melting of bulk non-ferrous metallic materials by microwave hybrid heating (MHH) and conventional heating: a comparative study on energy consumption. *Journal of the Brazilian Society of Mechanical Sciences and Engineering.* 2018;40(1): 1.
10. Mishra RR, Sharma AK. A Review of Research Trends in Microwave Processing of Metal-Based Materials and Opportunities in Microwave Metal Casting. *Critical Reviews in Solid State and Materials Sciences.* 2016;41(3): 217–255.
11. Rawat S, Samyal R, Bedi R, Bagha AK. Comparative performance of various susceptor materials and vertical cavity shapes for selective microwave hybrid heating (SMHH). *Physica Scripta.* 2022;97(12): 125704.
12. Patel DK, Bhoi HS, Kumar N. Microwave Heating Capabilities of Different Susceptor Material: Experimental and Simulation Study. *Silicon.* 2022;14: 6621–6635.
13. Boiprav OV, Bogush VA, Lynkou LM. Electromagnetic radiation reflection, transmission and absorption characteristics of microwave absorbers based on dilatant liquids and powdered activated wood charcoal. *Materials Physics and Mechanics.* 2023;51(6): 127–134.
14. Bhatt SC, Ghetiya ND. Review on effect of tooling parameters on microwave processing of metallic materials with special emphasis on melting/casting application. *International Journal of Metalcasting.* 2022;16: 2097–2127.
15. Stalin B, Ravichandran M, Balasubramanian M, Chairman CA, Pritima D, Dhinakaran V. Processing of MMC through conventional sintering and spark plasma sintering process: A review. *IOP Conference Series: Materials Science and Engineering.* 2020;988(1): 012092.
16. Singh S, Gupta D, Jain V. Fabricating In Situ Powdered Nickel–Alumina Metal Matrix Composites Through Microwave Heating Process: A Sustainable Approach. *International Journal of Metalcasting.* 2021;15: 969–982.
17. Bhatt S, Suthar S, Mistry D, Ghetiya N. Experimental study on microwave Ex-situ casting of AA 6061. *Materials Today: Proceedings.* 2021;44(1): 1312–1315.
18. Gangwar V, Singh H, Kumar S. Influence of Process Parameter on Microstructure, Residual Stress, Microhardness and Porosity of AA-6063 Microwave Cast. *International Journal of Metalcasting.* 2022;16: 826–841.

19. Kaushal S. Microstructure and Tribological Characterization of Composite Castings Developed through In-situ Microwave Hybrid Heating. *Inter Metalcast.* 2022;16: 2150–2161.
20. Lingappa MS, Srinath MS, Amarendra HJ. Microstructural and mechanical investigation of aluminium alloy (Al 1050) melted by microwave hybrid heating. *Materials Research Express.* 2017;4(7): 076504.
21. Mishra RR, Sharma AK. On mechanism of in-situ microwave casting of aluminium alloy 7039 and cast microstructure. *Materials & Design.* 2016;112: 97–106.
22. Mishra RR, Sharma AK. Experimental investigation on in-situ microwave casting of copper. *IOP Conference Series: Materials Science and Engineering.* 2018;346: 012052.
23. Lingappa M S, Srinath M S, Amarendra H J. Microstructural Investigation and Characterization of Bulk Brass Melted by Conventional and Microwave Processing Methods. *Materials Science Forum.* 2017;890: 356–361.
24. Marahadige SL, Sridharmurthy SM, Jayraj AH, Mahabaleshwar US, Lorenzini G, Lorenzini E. Development of copper alloy by microwave hybrid heating technique and its characterization. *International Journal of Heat and Technology.* 2018;36(4): 1343–1349.
25. Ram VK, Nandwani S, Vardhan S, Bahl S, Samyal R, Bagha AK. Microwave casting of stainless still through microwave hybrid heating. *IOP Conference Series: Materials Science and Engineering.* 2022;1248: 012047.
26. Singh S, Gupta D, Jain V. Processing of Ni-WC-8Co MMC casting through microwave melting. *Materials and Manufacturing Processes.* 2018;33(1): 26–34.
27. Kumar R, Bhowmick H, Gupta D, Bansal S. Development and characterization of multiwalled carbon nanotube-reinforced microwave sintered hybrid aluminum metal matrix composites: An experimental investigation on mechanical and tribological performances. *Proceedings of the Institution of Mechanical Engineers, Part L: Journal of Materials: Design and Applications.* 2021;235(10): 2310–2323.
28. Pal J, Gupta D, Singh TP. Processing and characterization of SS316 based metal matrix composite casting through microwave hybrid heating. *Proceedings of the Institution of Mechanical Engineers, Part C: Journal of Mechanical Engineering Science.* 2022;236(20): 10508–10527.
29. Nandwani S, Vardhan S, Bahl S, Yadav AK, Samyal R, Bagha AK. Evaluating the dynamic characteristics of microwave-casted metal matrix composite material by using experimental modal analysis. *Proceedings of the Institution of Mechanical Engineers, Part E: Journal of Process Mechanical Engineering.* 2023;238(4): 1580–1590.
30. Kaushal S, Bohra S, Gupta D, Jain V. On Processing and Characterization of Cu–Mo-Based Castings Through Microwave Heating. *International Journal of Metalcasting.* 2020;15: 530–537.
31. Bykov NY, Obraztsov NV, Hvatov AA, Maslyaev MA, Surov AV. Hybrid modeling of gas-dynamic processes in AC plasma torches. *Materials Physics and Mechanics.* 2022;50(2): 287–303.
32. Tamang S, Aravindan S. 3D numerical modelling of microwave heating of SiC susceptor. *Applied Thermal Engineering.* 2019;162: 114250.
33. Mishra RR, Sharma AK. Multi-physics simulation of in situ microwave casting of 7039 Al alloy inside different applicators and cast microstructure. *Proceedings of the Institution of Mechanical Engineers, Part E: Journal of Process Mechanical Engineering.* 2019;233(3): 617–629.
34. Sharma MV, Nekraje G, Bhuvan V, Hebbale AM, Srinath MS. Simulation studies on melting characteristics of bulk alloy Al-1050 during in-situ microwave casting process. *Materials Today: Proceedings.* 2022;52: 407–412.
35. Bhatt SC, Ghetiya ND, Joshi M. Multiphysics simulation and validation of microwave melting characteristics of AA6061 by finite element analysis. *Advances in Materials and Processing Technologies.* 2021;8(3): 1557–1568.
36. Bhatt SC, Ghetiya ND. 3D Multiphysics simulation of microwave heating of bulk metals with parametric variations. *Chemical Engineering and Processing - Process Intensification.* 2023;184: 109271.
37. Pryor RW. *Multiphysics Modeling using COMSOL*. Jones and Bartlett; 2011.
38. Thakur A, Bedi R. Microwave joining of copper pipes using selective microwave hybrid heating process: Simulation and experimental study. *Materials Today Communications.* 2024;38: 108154.
39. Lin B, Li H, Chen Z, Zheng C, Hong Y, Wang Z. Sensitivity analysis on the microwave heating of coal: A coupled electromagnetic and heat transfer model. *Applied Thermal Engineering.* 2017;126: 949–962.
40. Liu S, Fukuoka M, Sakai N. A finite element model for simulating temperature distributions in rotating food during microwave heating. *Journal of Food Engineering.* 2013;115(1): 49–62.